Cell, Vol. 82, 1001–1011, September 22, 1995, Copyright © 1995 by Cell Press

Cloning and Functional Analysis of TipE, a Novel Membrane Protein That Enhances Drosophila *para* Sodium Channel Function

Guoping Feng,* Péter Deák,† Maninder Chopra, and Linda M. Hall
Department of Biochemical Pharmacology
State University of New York at Buffalo
Buffalo, New York 14260-1200

Summary

Voltage-dependent sodium channels are involved in the initiation and propagation of action potentials in many excitable cells. Here we report that *tipE*, a gene defined by a temperature-sensitive paralytic mutation in Drosophila, encodes a novel integral membrane protein that dramatically stimulates functional expression in Xenopus oocytes of the Drosophila sodium channel α subunit encoded by the *paralytic* (*para*) locus. Using a heat shock promoter to control *tipE*$^+$ gene expression in transgenic flies, we demonstrate that *tipE*$^+$ gene expression is required during pupal development to rescue adult paralysis. In addition, we demonstrate a role for the *tipE* gene product in adults.

Introduction

Neuronal excitability is mediated by voltage-sensitive ion channels that allow specific ions to cross cell membranes to generate action potentials. Voltage-dependent sodium channels are responsible for the initial rising phase of the action potential (Hille, 1992). They are large membrane glycoproteins composed of a large α subunit (230–280 kDa). In addition, one or two tightly associated, smaller (33–38 kDa) β subunits have been demonstrated for several vertebrate sodium channels (Catterall, 1992). The large α subunit forms the ion permeable pore, while the smaller subunits play key roles in the regulation of channel function (Isom et al., 1994).

One advantage of using a genetic approach in Drosophila to dissect the molecular components underlying neuronal membrane excitability is that it does not require any a priori information about the gene product. Therefore, this approach has the potential to identify gene products that would not be isolated by biochemical methods or homology cloning (reviewed by Wu and Ganetzky, 1992). Using this genetic approach, several temperature-sensitive paralytic mutants, including temperature-sensitive *paralysis* (*para*^{ts}; Suzuki et al., 1971), temperature-sensitive *no action potential* (*nap*^{ts}; Wu et al., 1978), *temperature-induced paralysis*, locus *E* (*tipE*; Kulkarni and Padhye, 1982), and temperature-sensitive *seizure* (*sei*^{ts}; Jackson et al., 1984, 1985), were identified as mutations affecting neuronal sodium channel activities (Jackson et al., 1984, 1986; O'Dowd and Aldrich, 1988; O'Dowd et al., 1989). The *para* gene encodes a sodium channel α subunit (Loughney et al., 1989), while *nap* encodes a DNA-binding protein that may regulate *para* gene expression or RNA processing (Kernan et al., 1991).

The *tipE* mutation is an ethylmethane sulfonate–induced recessive mutation causing homozygous *tipE* flies to paralyze rapidly at 38°C and to recover immediately when returned to 23°C (Kulkarni and Padhye, 1982). [^{3}H]saxitoxin binding studies show a 30%–40% reduction of sodium channel–binding activity in head membranes from *tipE* mutant flies (Jackson et al., 1986). Whole-cell patch–clamp studies of sodium currents from cultured embryonic neurons also reveal a 40%–50% reduction in sodium channel density from *tipE* mutants (O'Dowd and Aldrich, 1988).

The combination of *tipE* with *nap* or *para* results in unconditional lethality or partial lethality of the double mutants at temperatures in which single mutants survive (Ganetzky, 1986; Jackson et al., 1986). The synergistic interaction of *tipE* with *para* is allele dependent. Some combinations allow partial viability while others result in complete lethality. The observation that allele dependence is not correlated with the residual *para* function of the different alleles led to the speculation that the *tipE* gene product may physically interact with *para* (Ganetzky, 1986; Jackson et al., 1986). Surviving double mutants of *tipE* with either *para* or *nap* are very weak and exhibit enhanced temperature sensitivity for paralysis (Ganetzky, 1986; Jackson et al., 1986). The *tipE* and *nap* double mutants also display a greater reduction of saxitoxin-binding activity than either single-mutant homozygote (Jackson et al., 1986). All these data strongly suggest that *tipE* is functionally related to sodium channels.

The *tipE* gene maps to 64B2 on the third chromosome and is disrupted by the chromosome translocation *T(2;3) TE2* (Feng et al., 1995). Localization of this translocation breakpoint by chromosome walking led to the isolation of a 7.4 kb genomic DNA fragment that crosses the breakpoint. Germline transformation experiments revealed that the 7.4 kb genomic DNA is all that is necessary to rescue *tipE* paralysis. Northern blot analysis identified three overlapping candidate mRNAs for the *tipE* gene (5.4 kb, 4.4 kb, and 1.7 kb) within this 7.4 kb genomic DNA. Here we report the cloning and functional characterization of the *tipE* gene. It encodes a novel 50 kDa integral membrane protein. We show that the *tipE* gene product stimulates functional expression of *para* sodium channels in Xenopus oocytes. In addition, by use of a heat shock promoter to control *tipE* gene expression in transgenic flies, we demonstrate that the *tipE* gene is required during pupal development to rescue adult paralysis. We also show that the *tipE* gene has a function in adults that protects them against a heat-induced lethality.

*Present address: Department of Anatomy and Neurobiology, Washington University School of Medicine, St. Louis, Missouri 63110.

†Present address: Department of Genetics, Attila József University, 6726 Szeged, Hungary.

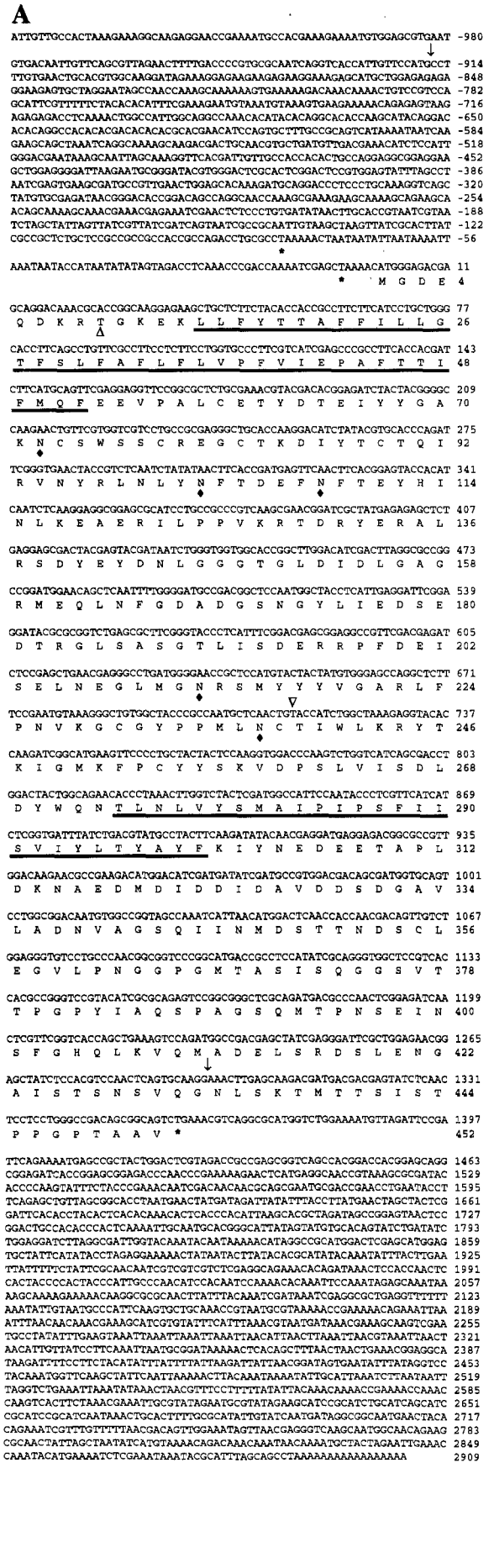

Figure 1. The *tipE*$^+$ cDNA Sequence

(A) Nucleotide sequence and deduced amino acid sequence of *tipE*$^+$. In-frame stop codons are indicated by asterisks. Proposed transmembrane domains are underlined. A potential protein kinase C phosphorylation site is indicated by an open triangle. Five potential N-glycosylation sites are marked by closed diamonds. The positions of introns are indicated by an arrow above the sequence. The open inverted triangle indicates the location of the point mutation in *tipE* mutant flies. (B) Hydrophobicity plot of the tipE deduced amino acid sequence. Regions above the line are hydrophobic. Transmembrane domains are indicated by arrows.

Results

Isolation of cDNA Clones and Genomic Organization

Previously, we described the identification of three overlapping candidate *tipE* transcripts (5.4 kb, 4.4 kb, and 1.7 kb) using probes from a 7.4 kb genomic DNA that rescues *tipE* paralysis (Feng et al., 1995). The abundant 4.4 kb and the much less abundant 5.4 kb mRNAs are predominantly expressed in heads and legs, while the 1.7 kb mRNA is mainly expressed in bodies (Feng et al., 1995). Fragments from the rescuing genomic DNA were used to screen a Drosophila head cDNA library. Three cDNA clones, corresponding to the 4.4 kb mRNA, were isolated, with the longest one having a 4 kb insert. Two partial clones, corresponding to the 5.4 kb mRNA, were also isolated by genomic DNA probes that hybridize specifically to the 5.4 kb mRNA. The cDNA clones corresponding to the 1.7 kb mRNA were obtained by reverse transcription–coupled polymerase chain reaction (RT–PCR) amplification of body mRNA by primers derived from the sequence of the 4 kb cDNA.

Comparison of sequence data from the cDNA clones and the genomic DNA fragment revealed that all three *tipE* candidate mRNAs are alternatively spliced forms of the same gene. The most abundant form (4.4 kb mRNA) consists of three exons. The 5.4 kb mRNA is an alternatively spliced form, with the intron between the first and second exon not spliced out. It may represent an incompletely processed transcript. Surprisingly, the 1.7 kb mRNA is an alternatively spliced form with only a few potential short open reading frames (ORFs) (encoding 37–48 amino acids). One possible explanation for this 1.7 kb transcript is that cells use a splicing mechanism to inactivate the gene when the *tipE* gene product is not needed. This is a well-characterized mechanism for a number of Drosophila genes (reviewed by Hodges and Bernstein, 1994), including *Sex lethal*, *transformer*, and *suppressor of white apricot*.

Analysis of cDNA Sequence and Deduced Amino Acid Sequence

The 4 kb cDNA clone that corresponds to the abundant 4.4 kb mRNA contains an ORF that encodes a deduced protein of 452 amino acids. This message contains a 1045 bp 5′ untranslated region and a 1549 bp 3′ untranslated region (Figure 1A). There are five consensus polyadenylation sequences (AATAAA) at positions 1824, 2053, 2490, 2664, and 2870, and there is a poly(A) tail at the 3′ end.

The ATG at position 1046 has been designated as the initial methionine start codon because it is preceded by two nearby in-frame stop codons. The four nucleotides immediately preceding the initial ATG (AAAC, positions −4 to −1) completely match the consensus sequence (C/A AA A/C) for initiation of translation in Drosophila (Cavener, 1987).

A database search using the deduced amino acid sequence revealed no significant sequence similarity to any other proteins. This novel protein has a calculated molecular mass of 50.2 kDa and is highly negatively charged, with an isoelectric point of 4.17. Aspartic acid and glutamic acid make up 14% of the total amino acids. The deduced protein sequence has two hydrophobic domains as judged by hydropathy analysis (Figure 1B; Kyte and Doolittle, 1982). The first hydrophobic domain contains 39 amino acids (from position 14 to position 52) preceded by a highly charged N-terminal sequence (8 out of 13 amino acids are charged). Although this hydrophobic domain is at the N-terminus, it is unlikely to function as a signal peptide for the following reasons: most eukaryotic signal peptide sequences are about 20 amino acids, with the longest being about 35 amino acids (von Heijne, 1985), whereas this domain would have 52 amino acids if cleaved as a signal peptide; sequence analysis does not give a predictable cleavage site using the −3 to −1 rule (von Heijne, 1986); in vitro translation in the presence of microsomes suggests that the N-terminal domain is not cleaved (see below). Therefore, we propose that this hydrophobic domain or a portion of it functions as a transmembrane domain. The second hydrophobic domain is from positions 274 to 300 (27 amino acids).

Other interesting features of this protein include a consensus site for potential protein kinase C phosphorylation of threonine at the N-terminus (position 9) and five potential N-glycosylation sites in the loop between the two transmembrane domains, at positions 72, 102, 108, 212, and 237.

The *tipE* Mutation Is a Premature Stop Codon in the ORF

To determine the molecular nature of the mutation in *tipE* flies, we sequenced, from *tipE* mutants, genomic DNA containing introns and the exons of the 4.4 kb mRNA. Comparison of sequences from mutant versus wild-type flies revealed a point mutation in nucleotide position 714 (Figure 1A). This T to A transversion mutation changes a cysteine codon (TGT) into a stop codon (TGA). This stop codon would result in a truncated protein of 237 amino acids and a predicted molecular mass of 27 kDa.

To exclude the possibility that the detected point mutation was a sequencing artifact, we noted that the putative mutation would eliminate an RsaI restriction enzyme site by changing the sequence from GTAC to GAAC. Digestion of PCR products amplified from mutant versus wild-type flies showed that the RsaI site was always missing from the mutant homozygotes but was always present in wild type (data not shown).

The Membrane Topology of TipE Protein

Hydropathy analysis of the deduced tipE protein predicted two hydrophobic segments long enough to span the plasma membrane (Figure 1B), suggesting that *tipE* encodes a transmembrane protein. To determine the transmembrane topology of this protein, we used in vitro translation in the presence of microsomes that allows membrane proteins to be translated, translocated, and glycosylated and to have their signal peptide sequences cleaved (Blobel and Dobberstein, 1975; Yost et al., 1983). As shown in lane 2 of Figure 2A, the molecular mass of in vitro translated tipE protein in the presence of microsomes is much larger (65 kDa) than that without microsomes (50 kDa; compare Figure 2A, lane 1). This increase in size is due to extensive glycosylation of the tipE protein since treatment of the sample with N-glycosidase F reduced the size back to the 50 kDa predicted from the deduced amino acid sequence (Figure 2A, lane 4). Since glycosylation occurs on the luminal side of the microsomes, this is good evidence that at least part of the protein is translocated into the lumen of microsomes (equivalent to the extracellular side in cells).

Integral membrane proteins can be distinguished from secretory or peripheral membrane proteins by treating the microsomes at high pH, which will extract vesicle contents (e.g., secretory proteins) as well as dissociate peripheral membrane proteins. This treatment does not remove integral membrane proteins (Fujiki et al., 1982; Gilmore and Blobel, 1985). As shown in lane 3 of Figure 2A, treatment of microsomes at high pH did not remove the tipE protein, although the same treatment did completely remove the control secretory protein β-lactamase (Figure 2C). These studies indicate that the tipE protein is an integral membrane protein.

To confirm the prediction that the first hydrophobic segment is not a signal peptide, we did the same in vitro translation experiment with the *tipE* mutant cDNA that produces a truncated protein lacking 36 amino acids of the proposed extracellular loop and also missing the second hydrophobic segment and the whole cytoplasmic C-terminus. This truncated protein has a predicted molecular mass of 27 kDa. As shown in lane 1 of Figure 2B, a truncated protein with a molecular mass of 27 kDa is found when the mutant mRNA is translated in the absence of microsomes. The size of the mutant protein increased to 39 kDa when translated in the presence of microsomes (Figure 2B, lane 2). As it is for the wild-type tipE protein, this increase in molecular mass is due to glycosylation of the protein since treatment of the sample with N-glycosidase F reduces the size back to the predicted 27 kDa (Figure 2B, lane 4). The extensive

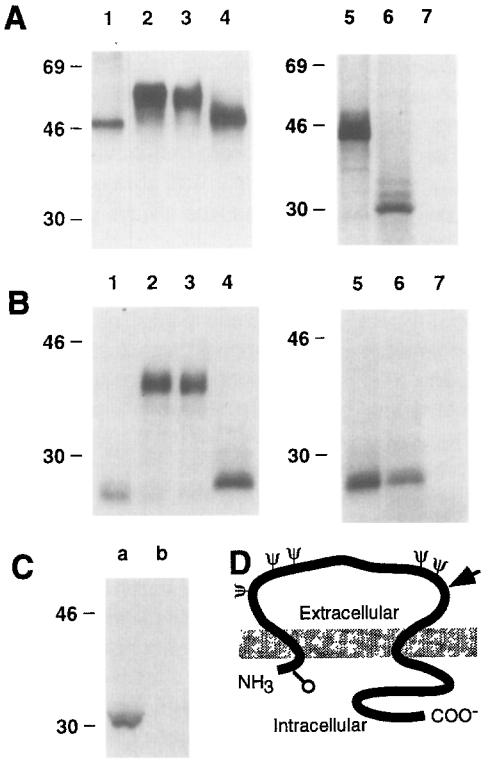

Figure 2. Membrane Topology of TipE Protein

(A and B) In vitro translation of *tipE*$^+$ mRNA (A) and *tipE* mutant mRNA (B) was performed in a rabbit reticulocyte lysate either in the absence (lane 1) or presence (lanes 2–7) of canine pancreatic microsomes. The translation products were either untreated (lanes 1 and 2) or treated with high pH (0.1 M Na_2CO_3 [pH 11.5]) (lane 3), N-glycosidase F (lanes 4 and 5), and proteinase K in the absence (lane 6) or presence (lane 7) of 0.1% Triton X-100 followed by N-glycosidase F treatment in both cases (lanes 6 and 7).

(C) β-Lactamase mRNA. This control mRNA encodes a secretory protein that should be removed by alkaline extraction. Lanes a and b show the product when translation occurred in the presence of microsomes. Lane b shows the effect of high pH treatment (0.1 M Na_2CO_3 [pH 11.5]).

(D) The predicted membrane topology of the tipE protein as confirmed by in vitro translation results. The open circle indicates a consensus protein kinase C phosphorylation site. Consensus sites for N-glycosylation are indicated by the psi symbols. The approximate location of the premature stop codon in the *tipE* mutant flies is indicated by the arrow.

glycosylation also indicates that the truncated loop is translocated into the lumen of the microsomes (extracellular in cells) since this is the only part in the truncated protein that contains potential N-glycosylation sites.

If the first hydrophobic domain is a signal peptide, it would be cleaved off when the message is translated in the presence of microsomes. The cleavage would reduce the protein size by 6 kDa (52 amino acids). The cleaved mutant protein would be secreted into the lumen of microsomes and removed at high pH because it would not have a transmembrane domain. As shown in Figure 2B, there is no size reduction of this truncated 27 kDa protein when translated in the presence of microsomes (compare the deglycosylated form in lane 4, translated in the presence of microsomes, with the nonglycosylated form in lane 1, translated in the absence of microsomes). Figure 2B also shows that this truncated protein is an integral membrane protein since treatment at high pH did not remove it from the microsomes (lane 3). These results strongly suggest that the first hydrophobic segment is a transmembrane domain.

The topology of membrane proteins can be predicted based on their signal peptides and transmembrane domains. Without a signal peptide, the predicted topology of the tipE protein would place both the N-terminus and the C-terminus intracellularly (Figure 2D), with the first transmembrane domain serving as the start–transfer signal and the second transmembrane domain as the stop–transfer signal (Wickner and Lodish, 1985). To test this model, we treated the in vitro translation product with proteinase K under conditions in which only the cytoplasmic domains would be accessible to the enzyme. If a fragment of the protein is translocated across the microsomal membrane into the lumen (equivalent to the extracellular side in cells), it would be protected from digestion by proteinase K. On the other hand, fragments extending outside of the microsomes (intracellular in cells) would be digested by proteinase K. As shown in Figure 2A, treatment with proteinase K reduced the size of the in vitro translated protein by about 17 kDa (from 50 kDa in lane 5 to 33 kDa in lane 6). This result is consistent with the C-terminus (16 kDa) and the N-terminus (1 kDa) being outside the microsomes (hence intracellular) and susceptible to proteinase K digestion. The size of the fragment protected from proteinase K digestion by the microsomal membrane (33 kDa; Figure 2A, lane 6) is consistent with the prediction that the loop between the two transmembrane domains is extracellular (26 kDa for the loop plus 7 kDa for the two transmembrane domains). The presence of Triton X-100, which disrupts the microsomal membrane, during proteinase K digestion completely eliminates the protective effect of the microsomal membranes (Figure 2A, lane 7). This confirms that the protection of the loop from proteinase K digestion is due to the translocation into the lumen of microsomes and is not due to insensitivity of the protein to proteinase K.

Treatment with proteinase K of microsomes containing in vitro translated truncated mutant protein also shows that the truncated loop is protected from proteinase K digestion (Figure 2B, lane 6), suggesting that the truncated loop is also translocated into the lumen of the microsomes. This is consistent with the results from the wild-type tipE protein. These results support the prediction that tipE is a membrane protein with two transmembrane domains and with both the N- and C-termini located intracellularly, as shown in Figure 2D.

Expression of *tipE* Is Neuronal and Is Developmentally Regulated

To determine where the *tipE* gene is expressed, we used a digoxigenin-labeled antisense DNA probe on whole mounts of stage 16 embryos. As shown in Figure 3A, *tipE*$^+$ mRNA is preferentially expressed in the central nervous system (CNS). Weak expression is also seen in the peripheral nervous system (PNS). The *para* gene (encoding a

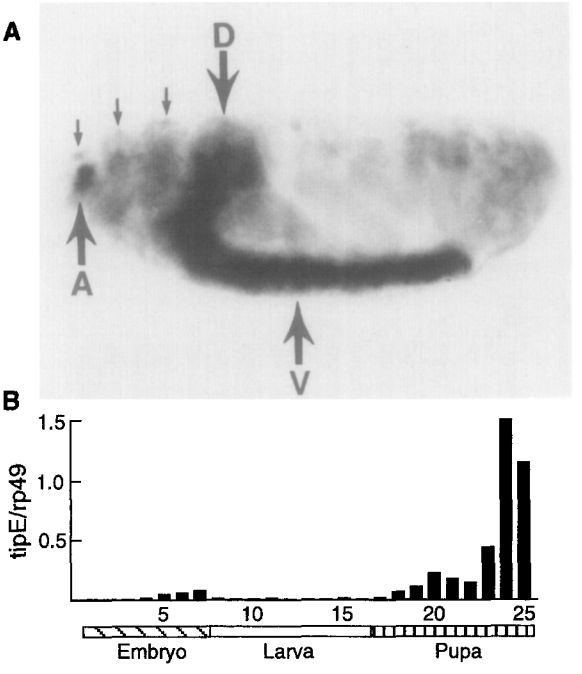

Figure 3. Spatial and Temporal Distribution of *tipE* Gene Expression

(A) Localization of *tipE*$^+$ mRNA in the embryonic nervous system by whole-mount in situ hybridization. Lateral view of a stage 16 (16–18 hr at 25°C) embryo hybridized with a single-stranded antisense *tipE*$^+$ DNA probe labeled with digoxigenin. Dorsal is up and anterior is to the left. Strong expression can be seen in the antennomaxillary complex (arrow marked A), dorsal cerebral hemispheres (arrow marked D), and ventral nerve cord (arrow marked V). Weak expression is also seen in the PNS (small arrows).

(B) Developmental regulation of the 4.4 kb mRNA of *tipE* gene. Wild-type samples were collected and staged at 25°C (Ashburner and Thompson, 1978). Poly(A)$^+$ RNA (10 μg) was loaded in each lane. Blots were probed with the cDNA fragment used in transformation rescue and reprobed with ribosomal protein 49 (*rp49*) to standardize for mRNA recovery and loading differences. The *rp49* cDNA encodes a ribosomal protein expressed throughout development (O'Connell and Rosbash, 1984). Signals on blots were quantitated using a Betascope blot analyzer (Betagen; Auron et al., 1987). Lanes 1–7 are embryonic mRNA: lane 1, 0–3 hr postoviposition; lane 2, 4–6 hr postoviposition; lane 3, 7–9 hr postoviposition; lane 4, 10–12 hr postoviposition; lane 5, 13–15 hr postoviposition; lane 6, 16–18 hr postoviposition; lane 7, 19–21 hr postoviposition. Lanes 8–16 are larval mRNA: lane 8, 22–24 hr postoviposition; lane 9, 25–36 hr postoviposition; lane 10, 37–48 hr postoviposition; lane 11, 49–60 hr postoviposition; lane 12, 61–72 hr postoviposition; lane 13, 73–84 hr postoviposition; lane 14, 85–96 hr postoviposition; lane 15, 97–108 hr postoviposition; lane 16, 109–120 hr postoviposition. Lanes 17–25 are pupal mRNA: lane 17, 0–12 hr postpuparium formation; lane 18, 13–24 hr postpuparium formation; lane 19, 25–36 hr postpuparium formation; lane 20, 37–48 hr postpuparium formation; lane 21, 49–60 hr postpuparium formation; lane 22, 61–72 hr postpuparium formation; lane 23, 73–84 hr postpuparium formation; lane 24, 85–96 hr postpuparium formation; lane 25, 97–108 hr postpuparium formation, as defined by Ashburner and Thompson (1978).

sodium channel α subunit) is expressed in both CNS and PNS throughout development (Hong and Ganetzky, 1994). As in the case of *para*, strong expression of the *tipE* gene is also seen in the antennomaxillary complex. These results suggest that *tipE* and *para* have similar general patterns of expression.

The temporal distribution of the *tipE* transcripts was analyzed quantitatively by using Northern blots of mRNA prepared from different developmental stages. Figure 3B shows the quantitation of standardized 4.4 kb *tipE*$^+$ mRNA in different developmental stages. There is a small peak of expression in middle to late stage embryos (Figure 3B, lanes 5–7) at 13–21 hr postoviposition (62%–100% embryonic development). Expression is dramatically increased in the pupal stage, especially in middle to late pupae (Figure 3B, lanes 20–25) at 44%–100% of pupal development. The high level of expression in the middle to late pupal stages suggests a role for the *tipE* gene in the newly remodeled, maturing adult nervous system.

tipE Gene Expression Is Required during Pupal Development to Rescue Adult Paralysis

To study the function of the *tipE* gene product in vivo, we did germline transformation with the ORFs of either the wild-type or mutant cDNA under the control of a heat shock promoter (Thummel and Pirrotta, 1992). To induce the gene expression, we gave a heat pulse of 1 hr at 35°C to homozygous transformant flies in a homozygous *tipE* background. To our surprise, heat shock of adult transformant flies containing wild-type cDNA failed to rescue the adult paralysis phenotype. Continuation of the heat shock process (once a day) for up to 2 weeks still did not rescue the paralysis.

To test the possibility that the *tipE* gene product might be needed during development, we gave a 1 hr heat pulse to transformants once a day throughout development until adult eclosion. Interestingly, the eclosed transformants with wild-type cDNA did not show temperature-induced paralysis after treatment throughout development. Moreover, no further heat pulse was needed after adult eclosion to maintain the rescue. That is, the paralysis phenotype is permanently "cured" by the induction of *tipE*$^+$ gene expression during development. As a control, transformants with *tipE* mutant cDNA failed to rescue paralysis following this same treatment regime.

To determine when *tipE* gene expression is required to rescue the adult paralysis, we induced *tipE* gene expression at different developmental stages by using an experimental paradigm similar to "shift-up" and "shift-down" experiments (Suzuki, 1970). In the shift-up experiment (Figure 4A), heat shocks were started at progressively later times of development and were continued once a day until adult eclosion. All heat-shocked flies were tested for temperature-induced paralysis following adult eclosion. This experiment determines the latest time during development when the start of *tipE*$^+$ gene expression will rescue adult paralysis. Starting the heat shock as late as 48 hr before eclosion (71% of pupal development) is enough to rescue adult paralysis completely.

In the shift-down experiment (Figure 4B), heat shocks were started 24 hr after egg laying. Every 24 hr a group of samples were removed from the treated group. This defines the earliest time during development when stopping expression of the *tipE*$^+$ gene does not affect the rescue of adult paralysis. The shift-down experiment showed that

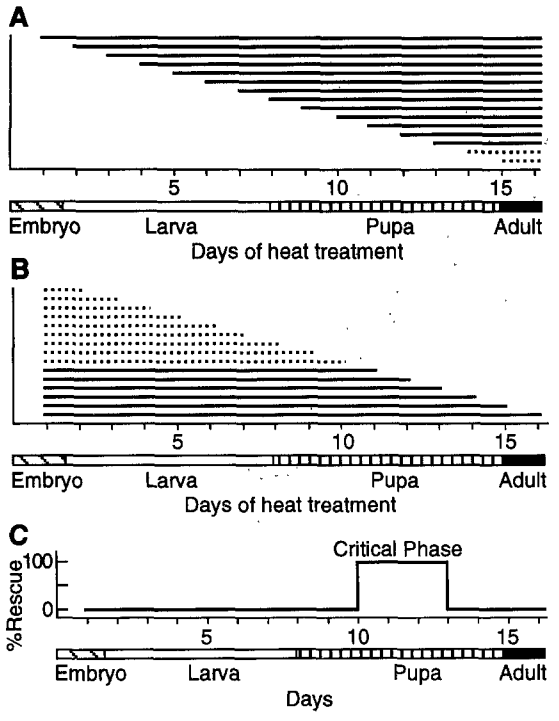

Figure 4. Rescue of *tipE* Paralysis by *tipE*$^+$ cDNA

To induce *tipE* gene expression, we collected eggs from homozygous *tipE* flies transformed with *tipE*$^+$ cDNA under the control of a heat shock promoter over a 1 hr period and subsequently heated them at 35°C for 1 hr; 50 eggs were used in each timepoint. Solid lines show treatments that rescue paralysis; dotted lines indicate treatments that failed to rescue.

(A) Shift-up experiment. Heat shocks were started at different times in development, as indicated by the start of the solid or dotted lines, and continued once a day until adult eclosion. Initial paralysis tests (38°C for 2 min) were conducted on adults within 12 hr of eclosion.

(B) Shift-down experiment. Heat shocks were started for all eggs at 24 hr after egg laying and continued every day. Every 24 hr a group was removed from the treated group. Flies were tested for paralysis as described above.

(C) Critical phase for the rescue of adult paralysis. The combination of shift-up and shift-down experiments defines a developmental window during which the expression of the *tipE*$^+$ gene is critical for the rescue of adult paralysis.

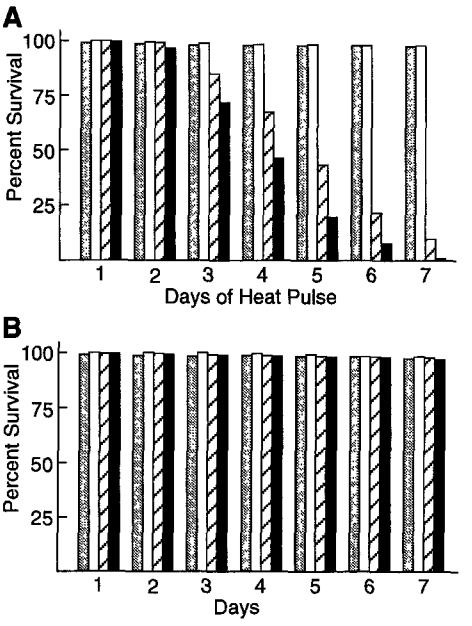

Figure 5. Rescue of Heat-Induced Lethality in Adult Flies

Adult flies grown at 21°C were collected within 12 hr of eclosion. Cross-hatched bars represent wild-type control flies. Open bars are *tipE* mutant flies transformed with wild-type *tipE* cDNA. Hatched bars are *tipE* mutant flies transformed with *tipE* mutant cDNA. Closed bars are *w;tipE se* flies. The total number of flies in each genotype in the heat-treated group (A) ranged from 471 to 1094 and in the control group (B) from 294 to 909. This experiment was repeated three times with similar results.

(A) Survival during heat shock treatment. A heat pulse of 35°C for 1 hr was given to adults once a day. This heat pulse served as a heat shock to induce the *tipE* gene expression in transformant flies and was also the factor that induced lethality in *tipE* mutants.

(B) Control experiments without heat shock treatment. All genotypes showed equivalent survival ranging from 96% to 99.1% over the total time of the experiment.

to rescue paralysis, the *tipE*$^+$ gene must be expressed beyond 72 hr postpuparium formation (43% of pupal development) (Figure 4B).

The combination of results from the shift-up and shift-down experiments defines a developmental window during which expression of the *tipE*$^+$ gene is essential to rescue adult paralysis (Figure 4C). To rescue adult paralysis, the *tipE* gene must be expressed during a critical phase, between 72 and 120 hr of postpuparium formation (43%–71% pupal development). Induction of *tipE* gene expression only during this critical phase (three heat pulses 24 hr apart) is enough to rescue adult paralysis completely (Figure 4C). However, a single heat shock within the critical phase failed to rescue paralysis completely, although partial rescue was observed. Partial rescue describes flies that did not paralyze completely in the standard test condition, but that were more debilitated than wild type. This shows that *tipE* gene expression is required over a period of several days in the maturing nervous system.

Expression of the *tipE* Gene in Adults Protects against a Heat-Induced Lethality

Figure 5A shows that repeated exposure of adults to heat pulses (35°C for 1 hr/day) causes lethality in *tipE* mutants (closed bars) but not in wild-type flies (cross-hatched bars). This defines another phenotype for the *tipE* mutation. Although repeated heat shock induction of *tipE* gene expression in adult transformants with *tipE*$^+$ cDNA failed to rescue the paralysis phenotype, it did completely rescue this heat-induced lethality (Figure 5A, open bars). This rescue occurred even though these flies were still paralyzed like homozygous mutants. This experiment shows that the *tipE*$^+$ gene plays an important role in adults, protecting against lethality due to heat stress.

We also tested flies transformed with *tipE* mutant cDNA in a *tipE* mutant background. Although these transformant flies did not rescue paralysis even if heat shocked throughout development, they show a lower heat-induced lethality (Figure 5A, hatched bars) compared with the nontrans-

formed *tipE* flies (closed bars). Therefore, overexpression of the truncated protein partially rescues heat-induced lethality in *tipE* flies, suggesting that the truncated tipE protein has some residual function.

TipE Protein Dramatically Enhances the Functional Expression of *para* Sodium Channels in Xenopus Oocytes

Although the *para* gene was cloned several years ago (Loughney et al., 1989), it has yet not been functionally expressed in an expression system. To determine whether the *tipE* gene product is required for *para* sodium channel function, we coinjected in vitro transcribed *tipE*$^+$ and *para*$^+$ RNA into Xenopus oocytes and recorded sodium currents by the 2-microelectrode voltage-clamp method.

Injection of *tipE*$^+$ RNA itself did not result in the expression of any current in Xenopus oocytes (data not shown), while the injection of 5 ng of *para*$^+$ RNA alone (Figure 6A) gave barely detectable sodium currents. However, when *para*$^+$ RNA was coinjected with *tipE*$^+$ RNA, sodium currents were greatly enhanced (~30-fold stimulation) (Figure 6B). As shown in Figure 6C, inward current first appears at −40 to −30 mV, and the peak current was observed at 0 mV. This voltage dependence of the expressed *para*$^+$–*tipE*$^+$ sodium currents is virtually identical to that seen for sodium currents recorded from cultured Drosophila embryonic neurons, where the current also appears first at −30 mV and the peak current is at 0 mV (O'Dowd and Aldrich, 1988).

Drosophila sodium channels in neurons are highly sensitive to tetrodotoxin (TTX), a sodium channel–specific blocker, and are blocked at 10 nM (O'Dowd and Aldrich, 1988). As shown in Figure 6D, the expressed *para*$^+$–*tipE*$^+$ sodium channels are also very sensitive to TTX, with a concentration that causes 50% inhibition (IC_{50}) of 0.2 nM. At 10 nM, TTX completely blocks the sodium current, which is again consistent with the results from cultured Drosophila embryonic neurons (O'Dowd and Aldrich, 1988).

In the absence of *tipE*$^+$, there is a very small but reproducible sodium current produced by 5 ng of *para*$^+$ RNA compared with the water-injected controls (Figure 6E). This current increased when 40 ng of *para*$^+$ RNA was injected (Figure 6F) and was blocked by 10 nM TTX (data not shown). Thus, *para*$^+$ RNA can produce low levels of sodium currents in the absence of *tipE*$^+$. An interesting question is whether the tipE protein simply enhances sodium channel expression or whether it also changes channel properties. This question is difficult to answer since *para*$^+$ RNA alone produces such low currents. In these experiments we find no significant difference in channel properties that can be attributed to the presence of *tipE*$^+$.

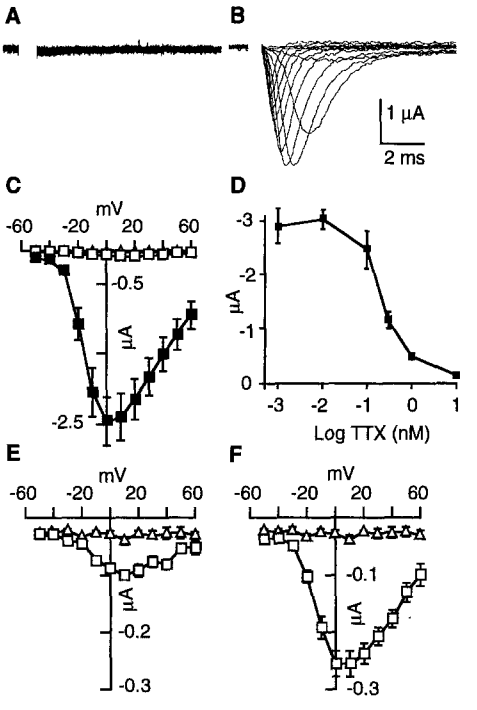

Figure 6. Coexpression of *tipE*$^+$ and *para*$^+$ RNA in Xenopus Oocytes

(A and B) Oocytes were injected with either 5 ng of *para*$^+$ RNA alone (A) or 5 ng each of *para*$^+$ and sense *tipE*$^+$ RNA (B). The currents shown were elicited by 20 ms voltage steps from a holding potential of −100 mV. The test potentials ranged from −50 mV to +60 mV in 10 mV increments. The transient capacitive currents have been blanked.

(C) The peak inward current versus test potential (I–V curve) was plotted from averaged data from >10 oocytes (each condition) injected with water (open triangles), 5 ng of *para*$^+$ RNA alone as in (A) (open squares), or 5 ng each of *para*$^+$ and *tipE*$^+$ RNA as in (B) (closed squares).

(D) TTX sensitivity of sodium channels expressed as in (B) was determined 5 min following bath application of TTX. Peak currents from five oocytes were used for each TTX concentration. Error bars show the standard error of the mean.

(E) Expanded scale replot of data from (C) showing difference between oocytes injected with water (open triangles) versus 5 ng of *para*$^+$ RNA (open squares).

(F) Oocytes injected with 40 ng of *para*$^+$ RNA alone (open squares) versus water (open triangles).

Discussion

The *tipE* Gene Product Dramatically Stimulates the Functional Expression of *para* Sodium Channels

Both ligand binding and electrophysiological studies suggest a reduction in functional sodium channels in *tipE* mutants (Jackson et al., 1986; O'Dowd and Aldrich, 1988). Two distinct sodium channel α subunits, para and DSC1, have been cloned from Drosophila. Since sodium channel α subunits in vertebrates are encoded by at least six distinct genes (Noda et al., 1986; Kayano et al., 1988; Rogart et al., 1989; Trimmer et al., 1989; Kallen et al., 1990; Gautron et al., 1992), additional sodium channel α subunits may exist in Drosophila. However, our sequence data clearly show that *tipE* does not encode another homolog of the voltage-dependent sodium channel α subunit (usually >150 kDa). Using the Xenopus oocyte expression system, we have shown that the tipE protein stimulates functional expression of *para* sodium channels. Very weak expression of *para* sodium currents in Xenopus oocytes is detected without the coinjection of *tipE*$^+$ RNA. These results, along with the fact that the tipE protein does not have significant sequence similarity to any protein currently available from the databases, suggest that the *tipE* gene defines a novel integral membrane protein that modulates *para* sodium channel function.

The *tipE* Gene Plays an Important Role in Development for Normal Function of the Adult Nervous System

Our transformation rescue results provide insight into the in vivo roles of the *tipE* gene in the nervous system. Using a heat shock promoter to control $tipE^+$ gene expression, we showed that the $tipE^+$ gene product is required during the middle to late pupal stage to rescue adult paralysis. Repeated induction of $tipE^+$ gene expression only in adult flies fails to rescue the paralysis. These results strongly suggest that the *tipE* gene plays an important role in the development of the nervous system during the period when the newly remodeled adult nervous system is undergoing maturation (Truman et al., 1993). Moreover, the rescue achieved by supplying the $tipE^+$ gene product during the pupal stage is permanent. No further $tipE^+$ gene expression is required after eclosion, suggesting that there might be defects of function, structure, or both in the adult nervous system caused by the lack of tipE protein during development. These defects can only be corrected by providing normal *tipE* function during development. Once these defects are corrected, the flies no longer show the temperature-sensitive paralytic phenotype even without continued, induced expression of the $tipE^+$ gene.

The functioning of the nervous system depends on precise patterns of neuronal connectivity. The development of these precise patterns involves pathfinding, target selection, and functional connection that are accomplished by the combination of two different mechanisms (reviewed by Goodman and Shatz, 1993): some require neuronal activity (activity dependent), and some do not (activity independent). The processes of pathfinding and target selection usually occur before neurons become active and therefore are activity independent, while the refinement and remodeling of these coarse patterns of synaptic connection into functional connections typically rely on neuronal activity. Studies from the vertebrate visual system showed that TTX can prevent the formation of the fine-grained retinotectal map without disrupting the axon growth and coarse connections (Meyer, 1982, 1983; Schmidt and Edwards, 1983; Fawcett and O'Leary, 1985; Kobayashi et al., 1990). A recent study showed that electrical activity is required for neuronal induction of transmitter receptor expression during synaptogenesis at embryonic neuromuscular junctions of Drosophila (Broadie and Bate, 1993). Using small patch mosaics, Burg et al. (1993) were able to study the activity-dependent development of sensory neurons in *para;nap* double mutants that are lethal at all temperatures. Although sensory cells in these double mutants are nonfunctional at all temperatures, their ultrastructure is normal. The branch pattern and terminal arborizations of central projections of these nonfunctional sensory cells are also normal. These findings led to the suggestion that although electrical activity may not be involved in pathfinding and ramification of terminal arborizations, it may be required for establishing and maintaining functional connectivity. Since *tipE* stimulates expression of *para* sodium currents, it is possible that defects in functional connectivity in the nervous system might occur in *tipE* mutants owing to a reduction in functional sodium channels at a critical time.

Truncated Protein in the *tipE* Mutant Has Residual Function

Sequencing genomic DNA from the *tipE* mutant revealed a point mutation causing a premature stop codon in the ORF of the *tipE* gene. The truncated protein has the first transmembrane domain and most of the large extracellular loop. This portion of the loop is properly translocated when translated in vitro. Using germline transformation with this mutant cDNA under the control of a heat shock promoter, we showed that although overexpression of the truncated protein failed to rescue the paralytic phenotype, it did partially rescue a heat-induced lethality in adult *tipE* flies. This result suggests that there is residual function in *tipE* flies and that, therefore, the *tipE* mutation is a hypomorph.

Although the translocation in *T(2;3)TE2* is accompanied by a 2.5 kb deletion at the 5′ end of the *tipE* gene, it only affects the upstream regulatory region and the 5′ untranslated region of the *tipE* gene and not the ORF. In a previous study (Feng et al., 1995), we showed that all three alternatively spliced forms of *tipE* transcripts are still expressed in *T(2;3)TE2* flies, but with smaller sizes and presumably with different expression patterns because of disruption of the upstream regulatory region. Thus, the null phenotype of *tipE* is unknown.

Possible Mechanisms by Which *tipE* Affects *para* Sodium Channel Functional Expression

Genetic studies showed that *tipE* and various *para* alleles interact synergistically in an allele-specific way that is not correlated to the residual activities of *para* sodium channels (Ganetzky, 1986). The simplest explanation is that *tipE* and *para* gene products physically interact and that the extent of the synergistic interaction is determined by the nature and the location of mutations in the different *para* alleles.

Sodium channels in vertebrate brains consist of a large (260 kDa) α subunit, a noncovalently linked β1 subunit (33 kDa), and a disulfide-linked β2 subunit (36 kDa) (Catterall, 1992; Isom et al., 1994). The β1 subunit of rat brain encodes an integral membrane protein with a single transmembrane domain (Isom et al., 1992). Coexpression of the β1 subunits with rat brain IIA α subunits increases the sodium current and modulates the inactivation kinetics to resemble that from intact neurons. The sequence of the β2 subunit has not yet been reported, but a model has been presented (Isom et al., 1994). Studies with specific anti-β2 antibody revealed that in developing rat brain neurons, 70% of the α subunits are not disulfide linked to β2 subunits (Schmidt et al., 1985; Schmidt and Catterall, 1986). These unassembled α subunits are full sized and are glycosylated like mature α subunits. However, they are located intracellularly and are nonfunctional. In contrast, all the α subunits located on the cell surface are disulfide linked to β2 subunits, suggesting that the β2 sub-

unit plays an important role in insertion, stabilization, or both of functional sodium channels in cell surface membranes.

Almost nothing is known about the subunit constitution of Drosophila sodium channels. The *tipE* gene does not have significant sequence similarity to the rat β1 subunit (Isom et al., 1992). Preliminary sequence data (Isom et al., 1994) suggest that rat brain β2 subunit also has a single transmembrane domain with a short intracellular C-terminus that is different from the proposed topology for the tipE protein. Immunoprecipitation with an anti-α subunit antibody revealed that disulfide-linked αβ2 subunits were present in the CNS of a broad range of vertebrates, including monkey, rat, chicken, frog, gecko, salmon, and eel (Wollner et al., 1987). However, an anti-β2 antibody generated with the purified rat brain β2 subunit only cross-reacted with the β2 subunits from monkey, rat, and chicken, suggesting that β2 subunits from other species are much less conserved or are different from those of monkey, rat, and chicken, although they are all disulfide linked to α subunits. The effect of *tipE* on the functional expression of *para* sodium channels in Xenopus oocytes makes *tipE* a possible candidate for a β2-like function in Drosophila.

Another possible way that *tipE* could affect the functional expression of *para* sodium channels in Xenopus oocytes is that, instead of acting as a subunit, tipE might be important for the proper folding and trafficking of the para protein. This is the mechanism for the effects of *neither inactivation nor afterpotential A* (*ninaA*), a mutation affecting phototransduction in Drosophila (Schneuwly et al., 1989; Colley et al., 1991; Stamnes et al., 1991). The *ninaA* gene encodes a transmembrane protein with high sequence similarity to peptidyl-prolyl *cis–trans* isomerases that catalyze protein folding by proline isomerization (Takahashi et al., 1989; Fischer et al., 1989). Mutation of the *ninaA* gene causes specific accumulation of a subset of rhodopsins, an integral membrane protein involved in phototransduction, in the endoplasmic reticulum, suggesting that *ninaA* is important for the proper folding and trafficking of rhodopsins from the endoplasmic reticulum to rhabdomeres (Colley et al., 1991; Stamnes et al., 1991). Further studies with specific antibodies against tipE and para will provide important insights into the role of *tipE* in *para* sodium channel functional expression.

Experimental Procedures

Drosophila Stocks

Drosophila cultures were grown at 21°C. The wild-type Canton S strain was obtained from J. C. Hall (Brandeis University). The *tipE sepia* (*se*) strain carries *tipE* (3–13.5) linked to *se* (3–26.0), a benign eye color mutation. Through repeated backcrossing of the *tipE se* strain to wild type for 10 generations, the *tipE* and *se* genes were placed in a wild-type genetic background.

Screening Libraries

A Drosophila head cDNA library provided by P. Salvaterra (Itoh et al., 1985) was screened with ^{32}P-labeled DNA probes (10^6 cpm/ml) under standard high stringency conditions (Sambrook et al., 1989).

DNA Sequencing and Data Analysis

Inserts from phage cDNA clones were subcloned into the pBluescript II SK(−) vector (Stratagene). Nested deletions (Henikoff, 1987) were subjected to double-stranded DNA sequencing (done at least twice in both directions) on an Applied Biosystems sequencer model 373A using the dideoxy chain termination method with fluorescent dye–tagged M13 or M13 reverse primers and the Taq dye primer sequencing kit (Applied Biosystems).

To sequence genomic DNA from wild-type and *tipE* mutants, we used sequence information from cDNA clones to synthesize primers with the M13 or SP6 sequence tagged to 5′ ends. Sequencing templates were generated by PCR by using genomic DNA from either wild-type or mutants as template, as previously described (Feng et al., 1995). PCR products were purified with Centricon 100 columns (Amicon) prior to sequencing. DNA contig assembly used Geneworks software (Intelligenetics, Incorporated). All other sequence analysis was done with GCG programs from the Wisconsin Genetics Computer Group (Devereux et al., 1984).

In Situ Hybridization to Embryo Whole Mounts

Whole-mount in situ hybridization to Drosophila embryos was done as described by Tautz and Pfeifle (1989). A 272 bp (positions 716–987 in Figure 1A) single-stranded digoxigenin-labeled cDNA probe was used as previously described (Zheng et al., 1995).

RNA Preparation and Northern Blots

Samples from different developmental stages were collected and synchronized at 25°C as described by Ashburner and Thompson (1978). Preparation of poly(A)$^+$ RNA, blots, and hybridization conditions were the same as previously described (Feng et al., 1995).

Germline Transformation

A 2 kb SspI fragment from the 4 kb cDNA clone was subcloned into the StuI site of pCaSpeR-hs vector containing a heat shock promoter (Thummel and Pirrotta, 1992). This SspI fragment contains the whole ORF, 67 bp of the 5′ untranslated region, and 558 bp of the 3′ untranslated region. Using RT–PCR, we generated a construct with the *tipE* point mutation by replacing the 638 bp KpnI–BstEII fragment (from nucleotides 570 to 1207) with the equivalent fragment amplified from *tipE* mutant flies. The construct and point mutation were confirmed by sequencing. Germline transformation was done as previously described (Feng et al., 1995).

In Vitro Translation

The SspI cDNA fragment used for germline transformation (see above) was subcloned into the EcoRV site of pBluescript II SK(−). A *tipE* mutant clone was generated as described for germline transformation. The constructs were linearized with SalI (for T3 RNA polymerase to make sense RNA) or with NotI (for T7 RNA polymerase to make antisense RNA as a control). To prepare *para* cRNA, the full-length cDNA construct in a pGEM-derived vector (pGH19) was linearized with NotI and transcribed with T7 polymerase. Transcripts were synthesized using mMESSAGEmMACHINE kits (Ambion), translated in vitro in a rabbit reticulocyte lysate (Promega) either in the presence or absence of canine pancreatic microsomes (Promega), and labeled with [^{35}S]methionine (at 0.8 mCi/ml; specific activity of 1016 Ci/mmol; Amersham). The translation product (5 μl or the equivalent after treatment) was analyzed by standard SDS–polyacrylamide gel electrophoresis. In some cases, the translation product was treated before being loaded onto gels. To treat at high pH, the translated product was incubated in 10 vol of 0.1 M Na_2CO_3 (pH 11.5) on ice for 30 min, then pelleted by centrifugation (80,000 × g for 15 min at 4°C), and rinsed with 10 vol of PBS (Gilmore and Blobel, 1985) before resuspension in gel loading buffer (Sambrook et al., 1989). For deglycosylation, 10 μl of translation product was treated with 1000 U of N-glycosidase F (New England Biolabs) in a 30 μl reaction using buffers and conditions recommended by manufacturer. For proteolytic treatment, 10 μl of translation product was incubated with proteinase K (10 μg/ml; Sigma) for 30 min at 0°C either in the presence or absence of 0.1% (v/v) Triton X-100.

Coexpression of *tipE* and *para* in Xenopus Oocytes

The *tipE*$^+$ (0.1 μg/μl) and *para*$^+$ (ranging from 0.1 to 0.8 μg/μl) RNAs were made as described for in vitro translation and mixed prior to injection into oocytes. *para*$^+$ cRNA includes 5′ and 3′ untranslated regions from the Xenopus β-globin message (from the pGH19 vector) to improve stability. Stage V oocytes from adult female Xenopus laevis were defolliculated with 2 mg/ml collagenase (type I, Sigma) in OR2 solution (82.5 mM NaCl, 2.0 mM KCl, 1.0 mM $MgCl_2$, and 5.0 mM HEPES [pH 7.5]) for 40 min. Defolliculated oocytes were injected with 50 nl of in vitro transcribed RNA and were recorded after 3–5 days at 20°C in 0.5× L-15 medium (Sigma) containing 10 μg/ml each of penicillin G, streptomycin, and gentamycin.

Sodium currents in oocytes were examined by 2-electrode voltage clamp (Krafte et al., 1988). The voltage and current electrodes (between 0.1 and 1 MΩ) were filled with 1% agarose in 1 M KCl (Schreibmayer et al., 1994). The bath solution contained 96 mM NaCl, 1.8 mM $CaCl_2$, 2.0 mM KCl, 1.0 mM $MgCl_2$, and 5.0 mM HEPES (pH 7.5). Leak subtraction was done by the on-line P/4 procedure (Bezanilla and Armstrong, 1977).

Acknowledgments

Correspondence should be addressed to L. M. H. We thank Jeffrey Warmke, Peiyi Wang, and Lex Van der Ploeg (Merck Research Laboratories, Rahway, New Jersey) and Robert Reenan and Barry Ganetzky (University of Wisconsin at Madison) for providing the *para* cDNA clone and Jeffrey Warmke and Joe Arena (Merck Research Laboratories, Rahway, New Jersey) for performing the initial *para–tipE* coexpression studies in Xenopus oocytes. Excellent assistance was provided by Jane Pursey-Lee for DNA sequencing and oligonucleotide synthesis and by Diying Yao in collection and analysis of data for Figure 5. We thank Drs. Frances Hannan and Jeffrey C. Hall for critical comments on the manuscript. This work was supported by a National Institutes of Health Jacob Javits Neuroscience Investigator Award (NS16204) to L. M. H.; G. F. was supported in part by fellowships from the Pharmaceutical Manufacturers Association Foundation, the Grass Foundation, and the Mark Diamond Research Fund of the Graduate Student Association of the State University of New York at Buffalo.

Received May 31, 1995; revised July 25, 1995.

References

Ashburner, M., and Thompson, J. N., Jr. (1978). The laboratory culture of *Drosophila*. In The Genetics and Biology of *Drosophila*, Volume 2a, M. Ashburner and T. R. F. Wright, eds. (New York: Academic Press), pp. 1–109.

Auron, P. E., Bolon, C., Quigley, G. J., Stanchfield, J. E., Sullivan, D. E., and Watkins, P. (1987). The nucleic acid blot analyzer. I. High speed imaging and quantitation of ^{32}P-labeled blots. Biotechniques *5*, 672–678.

Bezanilla, F., and Armstrong, C. M. (1977). Inactivation of the sodium channel. I. Sodium current experiments. J. Gen. Physiol. *70*, 549–566.

Blobel, G., and Dobberstein, B. (1975). Transfer of proteins across membranes. II. Reconstitution of functional rough microsomes from heterologous components. J. Cell Biol. *67*, 852–862.

Broadie, K., and Bate, M. (1993). Activity-dependent development of the neuromuscular synapse during Drosophila embryogenesis. Neuron *11*, 607–619.

Burg, M. G., Hanna, L., Kim, Y.-T., and Wu, C.-F. (1993). Development and maintenance of a simple reflex circuit in small-patch mosaics of *Drosophila*: effects of altered neuronal function and developmental arrest. J. Neurobiol. *24*, 803–823.

Catterall, W. A. (1992). Cellular and molecular biology of voltage-gated sodium channels. Physiol. Rev. *72*, S15–S48.

Cavener, D. R. (1987). Comparison of the consensus sequence flanking translational start sites in *Drosophila* and vertebrates. Nucl. Acids Res. *15*, 1353–1361.

Colley, N. J., Baker, E. K., Stamnes, M. A., and Zuker, C. S. (1991). The cyclophilin homolog *ninaA* is required in the secretory pathway. Cell *67*, 255–263.

Devereux, J., Haeberli, P., and Smithies, O. (1984). A comprehensive set of sequence analysis programs for the VAX. Nucl. Acids Res. *12*, 387–395.

Fawcett, J. W., and O'Leary, D. D. M. (1985). The role of electrical activity in the formation of topographic maps in the nervous system. Trends Neurosci. *8*, 201–206.

Feng, G., Deák, P., Kasbekar, D. P., Gil, D. W., and Hall, L. M. (1995). Cytogenetic and molecular localization of *tipE*: a gene affecting sodium channels in *Drosophila melanogaster*. Genetics *139*, 1679–1688.

Fischer, G., Wittmann-Liebold, B., Lang, K., Kiefhaber, T., and Schmid, F. X. (1989). Cyclophilin and peptidyl-prolyl *cis–trans* isomerase are probably identical proteins. Nature *337*, 476–478.

Fujiki, Y., Hubbard, A. L., Fowler, S., and Lazarow, P. B. (1982). Isolation of intracellular membranes by means of sodium carbonate treatment: application to endoplasmic reticulum. J. Cell Biol. *93*, 97–102.

Ganetzky, B. (1986). Neurogenetic analysis of *Drosophila* mutations affecting sodium channels: synergistic effects on viability and nerve conduction in double mutants involving *tipE*. J. Neurogenet. *3*, 19–31.

Gautron, S., Dos Santos, G., Pinto-Henrique, D., Koulakoff, A., Gros, F., and Berwald-Netter, Y. (1992). The glial voltage-gated sodium channel: cell- and tissue-specific mRNA expression. Proc. Natl. Acad. Sci. USA *89*, 7272–7276.

Gilmore, R., and Blobel, G. (1985). Translocation of secretory proteins across the microsomal membrane occurs through an environment accessible to aqueous perturbants. Cell *42*, 497–505.

Goodman, C. S., and Shatz, C. J. (1993). Developmental mechanisms that generate precise patterns of neuronal connectivity. Cell/Neuron *72/10* (Suppl.), 77–98.

Henikoff, S. (1987). Unidirectional digestion with exonuclease III in DNA sequence analysis. Meth. Enzymol. *155*, 156–165.

Hille, B. (1992). Ionic channels of excitable membranes. (Sunderland, Massachusetts: Sinauer Associates).

Hodges, D., and Bernstein, S. I. (1994). Genetic and biochemical analysis of alternative RNA splicing. Adv. Genet. *31*, 207–281.

Hong, C. S., and Ganetzky, B. (1994). Spatial and temporal expression patterns of two sodium channel genes in *Drosophila*. J. Neurosci. *14*, 5160–5169.

Isom, L. L., De Jongh, K. S., Patton, D. E., Reber, B. F. X., Offord, J., Charbonneau, H., Walsh, K., Goldin, A. L., and Catterall, W. A. (1992). Primary structure and functional expression of the β1 subunit of the rat brain sodium channel. Science *256*, 839–842.

Isom, L., DeJongh, K. S., and Catterall, W. A. (1994). Auxiliary subunits of voltage-gated ion channels. Neuron *12*, 1183–1194.

Itoh, N., Salvaterra, P., and Itakura, K. (1985). Construction of an adult *Drosophila* head cDNA expression library with λgt11. Dros. Inf. Serv. *61*, 89.

Jackson, F. R., Wilson, S. D., Strichartz, G. R., and Hall, L. M. (1984). Two types of mutants affecting voltage-sensitive sodium channels in *Drosophila melanogaster*. Nature *308*, 189–191.

Jackson, F. R., Gitschier, J., Strichartz, G. R., and Hall, L. M. (1985). Genetic modifications of voltage-sensitive sodium channels in *Drosophila*: gene dosage studies of the *seizure* locus. J. Neurosci. *5*, 1144–1151.

Jackson, F. R., Wilson, S. D., and Hall, L. M. (1986). The *tipE* mutation of *Drosophila* decreases saxitoxin binding and interacts with other mutations affecting nerve membrane excitability. J. Neurogenet. *3*, 1–17.

Kallen, R. G., Sheng, Z. H., Yang, J., Chen, L. Q., Rogart, R. B., and Barchi, R. L. (1990). Primary structure and expression of a sodium channel characteristic of denervated and immature rat skeletal muscle. Neuron *4*, 233–242.

Kayano, T., Noda, M., Flockerzi, V., Takahashi, H., and Numa, S. (1988). Primary structure of rat brain sodium channel III deduced from the cDNA sequence. FEBS Lett. *228*, 187–194.

Kernan, M. J., Kuroda, M. I., Kreber, R., Baker, B. S., and Ganetzky,

B. (1991). *nap*^{ts}, a mutation affecting sodium channel activity in Drosophila, is an allele of *mle*, a regulator of X chromosome transcription. Cell *66*, 949–959.

Kobayashi, T., Nakamura, H., and Yasuda, M. (1990). Disturbance of refinement of retinotectal projection in chick embryos by tetrodotoxin and grayanotoxin. Dev. Brain Res. *57*, 29–35.

Krafte, D. S., Snutch, T. P., Leonard, J. P., Davidson, N., and Lester, H. A. (1988). Evidence for the involvement of more than one mRNA in controlling the inactivation process of rat and rabbit brain Na channels expressed in *Xenopus* oocytes. J. Neurosci. *8*, 2859–2868.

Kulkarni, S. J., and Padhye, A. (1982). Temperature-sensitive paralytic mutations on the second and third chromosomes of *Drosophila melanogaster*. Genet. Res. *40*, 191–199.

Kyte, J., and Doolittle, R. F. (1982). A simple method for displaying the hydropathic character of a protein. J. Mol. Biol. *157*, 105–132.

Loughney, K., Kreber, R., and Ganetzky, B. (1989). Molecular analysis of the *para* locus, a sodium channel gene in Drosophila. Cell *58*, 1143–1154.

Meyer, R. L. (1982). Tetrodotoxin blocks the formation of ocular dominance columns in goldfish. Science *218*, 589–591.

Meyer, R. L. (1983). Tetrodotoxin inhibits the formation of refined retinotopography in goldfish. Dev. Brain Res. *6*, 293–298.

Noda, M., Ikeda, T., Kayano, T., Suzuki, H., Takeshima, H., Kurasaki, M., Takahashi, H., and Numa, S. (1986). Existence of distinct sodium channel messenger RNAs in rat brain. Nature *320*, 188–192.

O'Connell, P., and Rosbash, M. (1984). Sequence, structure, and codon preference of the *Drosophila* ribosomal protein 49 gene. Nucl. Acids Res. *12*, 5495–5513.

O'Dowd, D. K., and Aldrich, R. W. (1988). Voltage–clamp analysis of sodium channels in wild-type and mutant *Drosophila* neurons. J. Neurosci. *8*, 3633–3643.

O'Dowd, D. K., Germeraad, S. E., and Aldrich, R. W. (1989). Alterations in the expression and gating of Drosophila sodium channels by mutations in the *para* gene. Neuron *2*, 1301–1311.

Rogart, R. B., Cribbs, L. L., Muglia, L. K., Kephart, D. D., and Kaiser, M. W. (1989). Molecular cloning of a putative tetrodotoxin-resistant rat heart Na^+ channel isoform. Proc. Natl. Acad. Sci. USA *86*, 8170–8174.

Sambrook, J., Fritsch, E. F., and Maniatis, T. (1989). Molecular Cloning: A Laboratory Manual, Second Edition (Cold Spring Harbor, New York: Cold Spring Harbor Laboratory Press).

Schmidt, J. T., and Edwards, D. L. (1983). Activity sharpens the map during the regeneration of the retinotectal projection in goldfish. Brain Res. *269*, 29–39.

Schmidt, J. W., and Catterall, W. A. (1986). Biosynthesis and processing of the α subunit of the voltage-sensitive sodium channel in rat brain neurons. Cell *46*, 437–445.

Schmidt, J. W., Rossie, S., and Catterall, W. A. (1985). A large intracellular pool of inactive Na channel α subunits in developing rat brain. Proc. Natl. Acad. Sci. USA *82*, 4847–4851.

Schneuwly, S., Shortridge, R. D., Larrivee, D. C., Ono, T., Ozaki, M., and Pak, W. L. (1989). *Drosophila ninaA* gene encodes an eye-specific cyclophilin (cyclosporine A binding protein). Proc. Natl. Acad. Sci. USA *86*, 5390–5394.

Schreibmayer, W., Lester, H. A., and Dascal, N. (1994). Voltage clamping of *Xenopus laevis* oocytes utilizing agarose–cushion electrodes. Pflügers Arch. *426*, 453–458.

Stamnes, M. A., Shieh, B.-H., Chuman, L., Harris, G. L., and Zuker, C. S. (1991). The cyclophilin homolog ninaA is a tissue-specific integral membrane protein required for the proper synthesis of a subset of Drosophila rhodopsins. Cell *65*, 219–227.

Suzuki, D. T. (1970). Temperature-sensitive mutations in *Drosophila melanogaster*. Science *170*, 695–706.

Suzuki, D. T., Grigliatti, T., and Williamson, R. (1971). Temperature-sensitive mutations in *Drosophila melanogaster*. VII. A mutation (*para*^{ts}) causing reversible adult paralysis. Proc. Natl. Acad. Sci. USA *68*, 890–893.

Takahashi, N., Hayano, T., and Suzuki, M. (1989). Peptidyl-prolyl *cis–trans* isomerase is the cyclosporin A–binding protein cyclophilin. Nature *337*, 473–475.

Tautz, D., and Pfeifle, C. (1989). A non-radioactive *in situ* hybridization method for the localization of specific RNAs in *Drosophila* embryos reveals translational control of the segmentation gene *hunchback*. Chromosoma *98*, 81–85.

Thummel, C. S., and Pirrotta, V. (1992). New pCaSpeR P element vectors. Dros. Inf. Serv. *71*, 150.

Trimmer, J. S., Cooperman, S. S., Tomiko, S. A., Zhou, J., Crean, S. M., Boyle, M. B., Kallen, R. G., Sheng, Z., Barchi, R. L., Sigworth, F. J., Goodman, R. H., Agnew, W. S., and Mandel, G. (1989). Primary structure and functional expression of a mammalian skeletal muscle sodium channel. Neuron *3*, 33–49.

Truman, J. W., Taylor, B. J., and Awad, T. A. (1993). Formation of the adult nervous system. In The Development of *Drosophila melanogaster*, Volume 2, M. Bate and A. Martinez Arias, eds. (Cold Spring Harbor, New York: Cold Spring Harbor Laboratory Press), pp. 1245–1275.

von Heijne, G. (1985). Signal sequences: the limits of variation. J. Mol. Biol. *184*, 99–105.

von Heijne, G. (1986). A new method for predicting signal sequence cleavage sites. Nucl. Acids Res. *14*, 4683–4690.

Wickner, W. T., and Lodish, H. F. (1985). Multiple mechanisms of protein insertion into and across membranes. Science *230*, 400–407.

Wollner, D. A., Messner, D. J., and Catterall, W. A. (1987). β2 subunits of sodium channels from vertebrate brain: studies with subunit-specific antibodies. J. Biol. Chem. *262*, 14709–14715.

Wu, C.-F., and Ganetzky, B. (1992). Neurogenetic studies of ion channels in *Drosophila*. In Ion Channels, Volume 3, T. Narahashi, ed. (New York: Plenum Press), pp. 261–314.

Wu, C.-F., Ganetzky, B., Jan, L. Y., Jan, Y.-N., and Benzer, S. (1978). A *Drosophila* mutant with a temperature-sensitive block in nerve conduction. Proc. Natl. Acad. Sci. USA *75*, 4047–4051.

Yost, C. S., Hedgpeth, J., and Lingappa, V. R. (1983). A stop transfer sequence confers predictable transmembrane orientation to a previously secreted protein in cell-free systems. Cell *34*, 759–766.

Zheng, W., Feng, G., Ren, D., Eberl, D. F., Hannan, F., Dubald, M., and Hall, L. M. (1995). Cloning and characterization of a calcium channel α1 subunit from *Drosophila melanogaster* with similarity to the rat brain type D isoform. J. Neurosci. *15*, 1132–1143.

GenBank Accession Number

The accession number for the sequence reported in this paper is U27561.